Magnetostatic Field for the Active Contour Model: A Study in Convergence

Xianghua Xie and Majid Mirmehdi
Department of Computer Science,
University of Bristol, Bristol BS8 1UB, England
{xie,majid}@cs.bris.ac.uk

Abstract

A new external velocity field for active contours is proposed. The velocity field is based on magnetostatics and hypothesised magnetic interactions between the active contour and image gradients. In this paper, we introduce the method and study its convergence capability for the recovery of shapes with complex topology and geometry, including deep, narrow concavities. The proposed active contour can be arbitrarily initialised. Level sets are used to achieve topological freedom. The proposed method is compared against shape recovery methods based on distance vector flow, constant flow, generalised version of GVF, geodesic GGVF, and curvature vector flow.

1 Introduction

Active contour based methods have been widely used for shape recovery due to their natural handling of shape variation, e.g. [1, 11, 5]. The design of an active contour model is generally application dependent and involves the consideration of three fundamental issues: (a) *Contour representation:* One needs to decide whether to use a parametric representation or a non-parametric, implicit representation. (b) *Object boundary description and stopping function design:* Enormous effort has gone into designing and improving the techniques involved. These take one of three forms: (image gradient) boundary based approaches e.g. [1], region based approaches e.g. [5], or those that bridge the two, e.g. [10]. (c) *Initialisation and convergence:* Even with the right choices in (a) and (b), it is difficult to achieve simple, automatic initialisation. Indeed, initialisation dependency is still an open challenge for the active contour model. There is also no guarantee that the snake can or will converge to the desired boundary. The ability to converge to complex geometries, e.g. non-convex shapes, is undoubtedly essential for successful localisation.

The focus of this paper is on the issues of initialisation and convergence. A novel representation for object boundaries based on magnetostatics is proposed. We hypothesise magnetic interactions between active contours and object boundaries, resulting in a magnetic field that can attract or push the active contours to object boundaries with arbitrary initialisation. This approach solves a traditionally difficult problem in active contour models in that it allows the contour reach concavities which are highly acute. To fully illustrate the convergence dexterity of the proposed method, we apply a simplified active contour model to *given boundaries* to recover the shapes. As different active

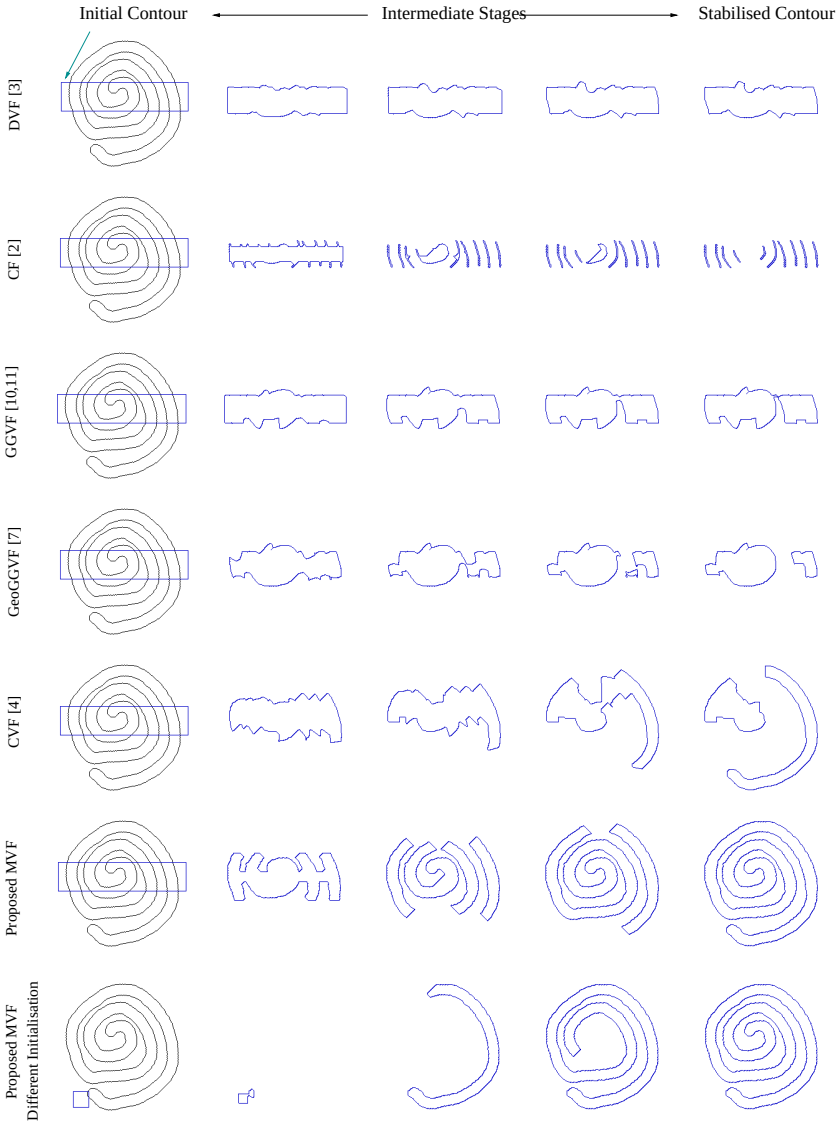

Figure 1: Swirl shape recovery - 1st column shows initial contours + swirl shape; 2nd-4th columns show intermediate stages (contour only); last column gives stabilised contours. Comparing active contours - 1st row: DVF [2]; 2nd row: CF [1]; 3rd row: GGVF [12, 11]; 4th row: GeoGGVF [6]; 5th row: CVF [3]; 6th row: the proposed MVF; last row: MVF with different initialisation.

contour models adopt different boundary extraction strategies and stopping function designs, by using given object boundaries, the comparison will be much more deterministic and avoids the ambiguity associated with parameter settings at the stages of image preprocessing, boundary extraction, and stopping function definition. Thus, this is a study in shape recovery only i.e. we ignore (b) above.

The proposed method is compared against five widely used external force fields: the

Euclidean distance field [2], the constant flow as in the geodesic active contour [1], the generalised version of GVF [12, 11], the geodesic GVF/GGVF [6], and curvature vector flow [3]. The work closest to this paper is by Gil and Radeva [3] in which they developed a new external velocity field derived from a distance map obtained by tracing back the propagation of the object boundary under modified curvature flows. This presents a way of adapting an active contour to non-convex shapes. We show that the proposed method outperforms all current state-of-the-art approaches, including [3]. The swirl example in Fig. 1 illustrates the power of the new method, as well as its initialisation invariance, compared to the techniques mentioned above.

Next, Section 2 gives a brief introduction to the five external velocity fields we compare against. The proposed method is described in Section 3. Experimental results and a comparative study appear in Section 4. Section 5 concludes the paper.

2 Background

The methods we shall compare against all have their own characteristics, plus advantages and disadvantages. Note that the usual contour regularisation terms, e.g. curvature flow, are not included in the formulae below, as they are not necessary for this study. In what follows, $f(\mathbf{x})$ is the image gradient (here includes the object boundary only) for each pixel position $\mathbf{x}$, and $\hat{\mathbf{N}}$ denotes the unit inward normal of the evolving contour.

• *Distance vector flow (DVF)* - The Euclidean distance transform $\mathscr{D}(\mathbf{x})$ is computed to find the nearest distance to the object boundary for each pixel position $\mathbf{x}$. In [2], Cohen and Cohen used the Chamfer distance, which approximates the Euclidean distance, to derive this external force for the active contour. The DVF is given as $-\nabla\mathscr{D}(\mathbf{x})$ with the active contour then stated as:

$$C_t = -(\nabla\mathscr{D}(\mathbf{x}) \cdot \hat{\mathbf{N}})\hat{\mathbf{N}}. \tag{1}$$

• *Constant flow (CF)* - The image dependent constant flow can be formulated as

$$C_t = g(\mathbf{x})\hat{\mathbf{N}}, \tag{2}$$

where $g(\mathbf{x}) = 1/(1+f(\mathbf{x}))$ and is commonly known as the stopping function. This flow shows each point on the contour moving in the direction of its normal at a speed proportional to $g(\mathbf{x})$. It monotonically shrinks or expands the contour towards the object boundary. It plays an important role in the geodesic snake model introduced by Caselles *et al.* [1], and used widely in incremental improvements, such as [8].

• *Generalised gradient vector flow (GGVF)* - The GVF [12] and its generalised version GGVF [11] introduced by Xu and Prince have been widely used in active contour models as external forces, e.g. [7]. The GGVF field, $\tilde{\mathbf{v}}(\mathbf{x})$, is defined as the equilibrium solution of the partial derivatives of:

$$\mathbf{v}_t(\mathbf{x}) = p(|\nabla f(\mathbf{x})|)\nabla^2\mathbf{v}(\mathbf{x}) - q(|\nabla f(\mathbf{x})|)(\mathbf{v} - \nabla f(\mathbf{x})), \tag{3}$$

where the initial vector field $\mathbf{v}(\mathbf{x}, t=0) = \nabla f(\mathbf{x})$, and $p(.)$ and $q(.)$ are monotonically non-increasing and non-decreasing functions respectively, controlling the amount of diffusion. These two functions are selected such that $p(.)$ gets smaller as $q(.)$ becomes larger with the desired result that in the proximity of large gradients, there will be very

little smoothing and the vector field will be nearly equal to $\nabla f(\mathbf{x})$:

$$p(|\nabla f(\mathbf{x})|) = e^{-\frac{|\nabla f(\mathbf{x})|}{K}}, \quad q(|\nabla f(\mathbf{x})|) = 1 - p(|\nabla f(\mathbf{x})|), \tag{4}$$

where K is a constant and acts as a trade-off between field smoothness and gradient conformity. The GGVF active contour for our shape recovery study can then be defined as:

$$C_t = (\tilde{\mathbf{v}}(\mathbf{x}) \cdot \hat{\mathbf{N}})\hat{\mathbf{N}}. \tag{5}$$

• *Geodesic GVF/GGVF (GeoGVF/GeoGGVF)* - Recently, Paragios *et al.* [6] integrated the GVF with the geodesic active contour model, referred to here as GeoGVF. The GVF provides the bidirectional force to drive the contours towards edges, while the constant flow from the geodesic model poses conditional inflation or deflation forces on the contour. The two forces are mutually exclusive [6]:

$$C_t = [(1 - |H(\mathbf{x})|)\tilde{\mathbf{v}}(\mathbf{x}) \cdot \hat{\mathbf{N}} + H(\mathbf{x})]\hat{\mathbf{N}}, \tag{6}$$

where the weighting function $H(\mathbf{x}) = sign(\tilde{\mathbf{v}}(\mathbf{x}) \cdot \hat{\mathbf{N}})e^{-\delta|\tilde{\mathbf{v}}(\mathbf{x}) \cdot \hat{\mathbf{N}}|}$, and δ is a scale factor. The additional adaptive bidirectional constant force is designed to determine the curve propagation when the GVF term becomes inactive, i.e. gradient vectors are tangent to contours. GGVF generally outperforms GVF [11], and as such we implement this method with GGVF instead of GVF. We shall refer to it as GeoGGVF.

• *Curvature vector flow*[1] *(CVF)* - Gil and Radeva [3] proposed a new distance transform based on the mean curvature flow to attract contours into shape concavities. Their principal idea was to evolve the object boundaries according to curvature flow till they were no longer concave. The inward or outward propagation was defined by monotonically non-negative or non-positive curvature flow:

$$\begin{cases} f_t = \max(\kappa, 0)\hat{\mathbf{N}} & \text{inward propagation,} \\ f_t = \min(\kappa, 0)\hat{\mathbf{N}} & \text{outward propagation,} \end{cases} \tag{7}$$

where κ denotes the curvature. A distance map $\mathscr{D}^{\kappa}(\mathbf{x})$ was then obtained by tracing back the evolution of the boundary from which the curvature vector flow, $-\nabla\mathscr{D}^{\kappa}(\mathbf{x})$, was derived. The CVF active contour then evolved as:

$$C_t = -(\nabla\mathscr{D}^{\kappa}(\mathbf{x}) \cdot \hat{\mathbf{N}})\hat{\mathbf{N}}. \tag{8}$$

Methods that rely directly on the boundary gradient inevitably have very limited capture range and are not able to reach concavities. Using the distance transform to obtain a DVF was one attempt to enlarge the capture range [2], but this still has difficulties with concave shapes. Caselles *et al.* [1] introduced the CF into the geometric active contour model to speed up its convergence and to pull or push the active contour towards object boundaries. However, this can only monotonically expand or shrink the contour. Xu and Prince [11, 12] iteratively diffused the edge gradient vector to homogeneous regions to significantly enlarge the capture range and increase the ability to reach concavities (but not sufficiently). Their GVF/GGVF active contour fails to converge when the contour is tangent to the velocity vector. This can be demonstrated using the four-disc problem in

[1] Note that the curvature vector flow is different from the well-known curvature flow.

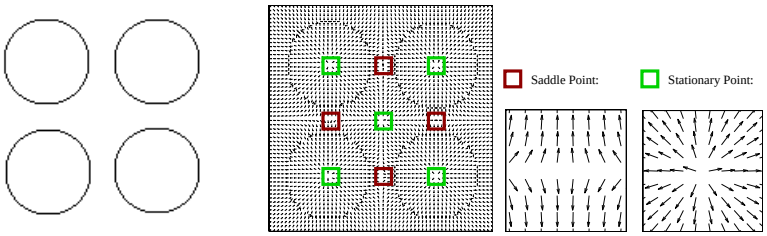

Figure 2: The four-disc problem - from left: An image contains four disc boundaries, the GGVF velocity map, enlarged saddle point (red square) and stationary point (green square).

Fig. 2 where there are four saddle points (indicated in dark red) and five stationary points (in light green) in the GGVF velocity map (final results in Fig. 5).

Several attempts have been made to solve the convergence issue. Gil and Radeva [3] proposed the CVF, derived from a curvature dependent distance transform, to push the active contour into concavities. However, this only reduces the number of stationary or saddle points, and can not completely eliminate them. Moreover, *it requires there be no gaps in the object boundary*. Paragios *et al.* [6] added the constant flow to the GVF model which pushes the active contour when it is close to tangent to the underlying vector. This still can not solve the four-disc problem as the conditionally added constant force can not overcome the stationary point in the centre of the four discs which will prevent the contour from further propagation. Very recently, Li *et al.* [4] suggested the active contour be split along those stationary and saddle points. This strategy is not appropriate when the active contour is placed inside the object or crosses the object boundary.

The proposed method, described next, shows significant improvements on all the above techniques.

3 Proposed Method

Our approach is to define a new external force based on magnetostatics. In brief, we hypothesis electric currents flowing through both the object boundary and the active contour. The magnetic fields generated by each of the currents will interact and cause a force between them. This magnetic vector force (MVF) field behaves as an external force to push or pull the active contour towards the object boundary. Next, we present the basic theory of magnetostatics, based on which the MVF active contour is then presented.

3.1 The magnetostatic field

Consider two points P and Q with charges, q_P and q_Q, and velocity vectors $\mathbf{u}_P$ and $\mathbf{u}_Q$ respectively. The magnetostatic force exerted upon q_P due to q_Q is [9]:

$$\mathbf{F}_{QP} = q_P \mathbf{u}_P \times \mathbf{B}_P, \qquad \mathbf{B}_P = \mu_0 q_Q \mathbf{u}_Q \times \frac{\hat{\mathbf{R}}_{QP}}{4\pi R_{QP}^2}, \tag{9}$$

where $\mathbf{B}_P$ is known as the magnetic flux density at point P due to the point charge at Q, μ_0 is the permeability constant, R_{QP} is the distance between the two charges, $\hat{\mathbf{R}}_{QP}$ is their unit distance vector, and $\times$ denotes the cross product. The magnetic field $\mathbf{H}$ is then defined as $\mathbf{H} = \mu_0^{-1}\mathbf{B}_P$. It is clear that $q\mathbf{u}$ can be viewed as an elementary current introduced by a

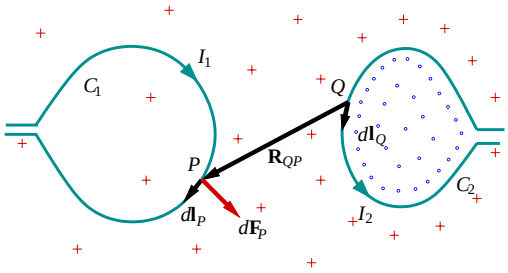

Figure 3: Magnetic force between two currents - see text for details.

moving charge. In order to obtain the magnetic field introduced by a current, we consider infinitesimal current segments $d\mathbf{l}_P$ and $d\mathbf{l}_Q$ at P and Q on loops C_1 and C_2 respectively (see Fig. 3). The total force on $d\mathbf{l}_P$ due to current I_2 is then:

$$d\mathbf{F}_P = I_1 d\mathbf{l}_P \times \mathbf{B}_P, \tag{10}$$

where $\mathbf{B}_P$ is:

$$\mathbf{B}_P \equiv \frac{\mu_0}{4\pi} I_2 \oint_{C_2} d\mathbf{l}_Q \times \frac{\hat{\mathbf{R}}_{QP}}{R_{QP}^2}, \tag{11}$$

which is commonly known as the Biôt-Savart Law. It defines how the magnetic flux density is obtained from a given current. In Fig. 3, the red '$+$' denotes the magnetic field going perpendicularly into the image plane and '$\cdot$' denotes the magnetic field coming out of the image plane. These symbols represent the overall magnetic field due to current I_2. The magnetic force $d\mathbf{F}_P$ at position P on C_1 is in its outward normal direction. Next, we show how to apply these principles to our active contour model.

3.2 MVF active contour

Magnetostatic theory is applied to our active contour model by charging both the object boundary and the active contour with electric currents. The concept is represented in Fig. 3 by treating C_1 as an active contour and C_2 as an object boundary. As we are interested in the deformation of the contours, only the forces exerted by the object boundary on the active contour are needed. In other words, we shall ignore magnetic forces introduced by the active contour. In order to do so, we need to obtain an estimation of the hypothesised direction of the currents in the object boundary and the active contour. We then compute the resulting magnetic flux density at each pixel position in the image using (11), based on which the active contour drives towards the object boundary according to (10).

The direction of the current can be estimated as the boundary orientation which can be computed using various techniques, e.g. by extracting the chain code. Here, we use the signed distance transform, $\mathscr{D}^{\pm}(\mathbf{x})$, the same as initialising a level set function. Let $\mathscr{D}_x^{\pm}(\mathbf{x})$ and $\mathscr{D}_y^{\pm}(\mathbf{x})$ be the partial derivatives in x and y. The boundary orientation can be conveniently obtained by a 90° rotation of the gradient vector field $(\mathscr{D}_x^{\pm}(\mathbf{x}), \mathscr{D}_y^{\pm}(\mathbf{x}))$. A clockwise rotation in the *image coordinates* gives an orientation vector field as:

$$\mathbf{O}(\mathbf{x}) = (-\mathscr{D}_y^{\pm}(\mathbf{x}), \mathscr{D}_x^{\pm}(\mathbf{x})). \tag{12}$$

In a similar fashion, the direction of the current for the active contour is given based on the estimation of the contour orientation. However, as we are using a level set representation, the active contour is already embedded in a 3D surface Φ, obtained from the

signed distance transform on the contour. Hence, no extra preparation is necessary, other than similarly rotating the gradient vector of the level set function, $\nabla\Phi$.

Thus, we can work out the magnetic flux density $\mathbf{B}(\mathbf{x})$ at each pixel position $\mathbf{x}$ due to the electric current applied to the object boundary. As only pixels on the object boundary will contribute to the magnetic field, $f(\mathbf{x})$ is reduced to $f(\mathbf{s})$, where $\mathbf{s}$ denotes a boundary pixel. So, given current $I_{f(\mathbf{s})}$, the magnetic flux density is computed as:

$$\mathbf{B}(\mathbf{x}) = \frac{\mu_0}{4\pi} \sum_{\mathbf{s} \in f(\mathbf{s})} I_{f(\mathbf{s})} d\mathbf{s} \times \frac{\hat{\mathbf{R}}_{\mathbf{xs}}}{R^2_{\mathbf{xs}}}, \tag{13}$$

where $d\mathbf{s}$ is the electric current vector at $\mathbf{s}$ on the object boundary $f(\mathbf{s})$, $\hat{\mathbf{R}}_{\mathbf{xs}}$ is the unit distance vector from $\mathbf{x}$ to $\mathbf{s}$, and $R_{\mathbf{xs}}$ is the distance between these two points. Note $I_{f(\mathbf{s})}$ is a constant for a given object boundary, so it can be removed from the sum.

Given the current I_C applied to the active contour C, its velocity field due to the magnetic field is:

$$\mathbf{F}(\mathbf{x}) = I_C d\mathbf{r} \times \mathbf{B}(\mathbf{x}), \tag{14}$$

where $d\mathbf{r}$ denotes the electric current vector on the active contour. Note that $\mathbf{F}(\mathbf{x})$ is always perpendicular to $d\mathbf{r}$, i.e., the velocity is always enforced in the contour normal inward or outward direction. Thus, the propagating contour will not suffer from saddle and stationary point related issues, e.g. it will successfully deal with the four-disc problem.

Given the velocity field $\mathbf{F}(\mathbf{x})$ derived from the magnetic interactions between the object boundary and the active contour, the evolving MVF active contour is defined as:

$$C_t = (\mathbf{F}(\mathbf{x}) \cdot \hat{\mathbf{N}})\hat{\mathbf{N}}. \tag{15}$$

Its level set representation then takes the following form:

$$\Phi_t = (-\mathbf{F}(\mathbf{x}) \cdot \frac{\nabla\Phi}{|\nabla\Phi|})|\nabla\Phi| = -\mathbf{F}(\mathbf{x}) \cdot \nabla\Phi. \tag{16}$$

From (1), (5), and (8), we can see that the velocity fields from DVF, GGVF, and CVF are static external forces. Their direction and magnitude are based on spatial position only, and not on the active contour; hence, the contour in those cases will not be able to propagate through saddle or stationary points. As for CF (see (2)), its direction is solely based on the active contour but its magnitude is based on the boundary. Thus, it can only monotonically expand or shrink and can not recover broken boundaries or be initialised across boundaries. The GeoGGVF, as in (6), is dominated by the external GGVF force, but will be conditionally influenced by a constant force imposed on the contour. However,

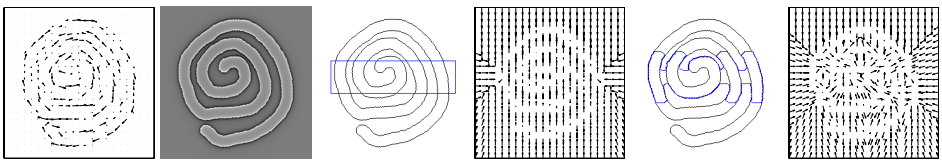

Figure 4: From left: estimated boundary orientation, magnitude of the magnetic field, initial active contour, initial external force field, evolving contour, and its associated external force field. Final result is shown in the penultimate row of Fig. 1.

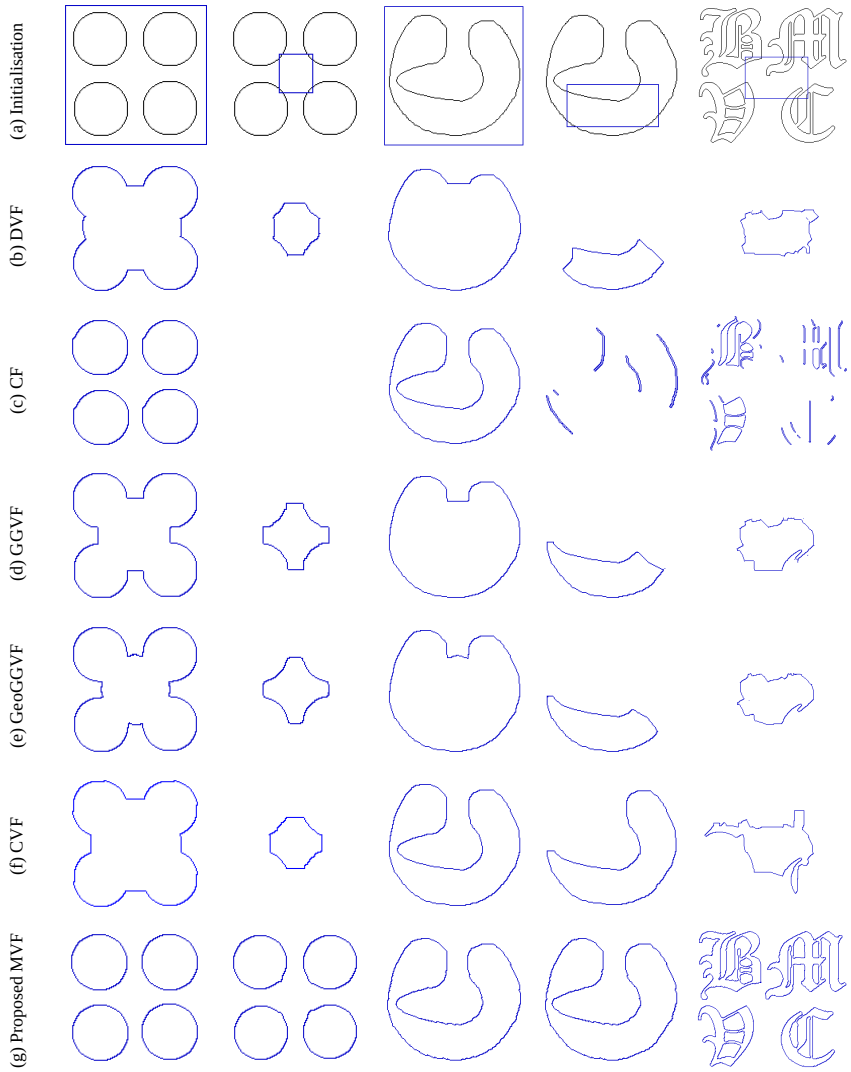

Figure 5: Convergence ability comparative study - row (a): Various shapes with initial active contours; row (b): results using DVF; row (c): results using CF; row (d): results using GGVF; row (e): results using GeoGGVF; row(f): results using CVF; row (g): results using proposed MVF.

as the direction of the constant force is mainly determined by the external vector flow, it still can not resolve the topological issues of the static external force.

The MVF has a distinctive feature in that its direction relies on both spatial position and the evolving contour. The external bidirectional velocity is dynamically adaptive based on contour position as shown in (14), and equally importantly its direction is always perpendicular to the evolving contour. The strength is determined by the magnitude of the magnetic field. Thus, the active contour can be initialised across the object boundary and reach into concave regions. Fig. 4 demonstrates MVF's adaptive external velocity field.

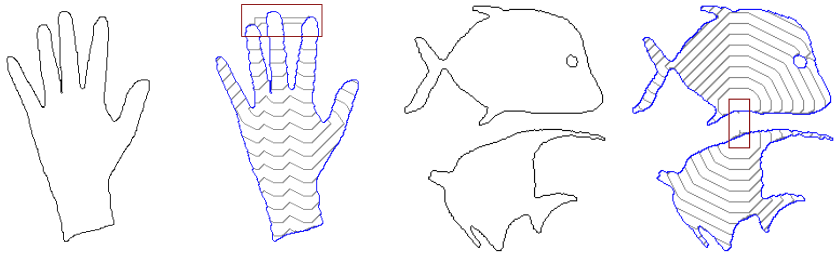

Figure 6: Recovering shapes with complex geometries with arbitrary initialisations.

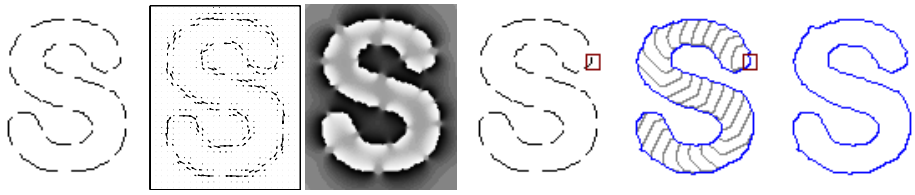

Figure 7: Recovering an object with broken boundaries - from left: initial shape with 23 boundary gaps, estimated boundary orientation using chain codes, magnitude of the magnetic field, initial active contour, evolving contours, and stabilised MVF active contour.

4 Experimental Results

In this section, we show comparative results on various shape geometries, different topologies, and objects with broken boundaries.

The four-disc problem: The first two columns in Fig. 5 show comparative results for solving the four-disc problem. When the initial contour was placed outside the four discs (first column), only CF and MVF could accurately localise them. However, in a more arbitrary initialisation case (cross-boundary in the second column), only MVF was successful. The saddle points and stationary points (see Fig. 2) prevented the other active contours from recovering the discs. Note the CF contour in this case simply disappeared.

Concave Shapes: Next, we compare the results on a concave shape, as shown in the third and fourth columns in Fig. 5, again with different initialisation conditions. The MVF active contour was again the only one which could successfully recover the shape in both cases. The other methods can neither handle arbitrary initialisations nor overcome the saddle point in the entrance of the concave shape. Note that the constriction on the left side of the concave shape causes severe problems for the CVF active contour.

Complex geometry: When dealing with complex geometries, MVF was the only model that managed to complete the task. Examples given in Fig. 1 and the last column of Fig. 5 demonstrate the superior performance of MVF. The latter example further illustrates MVF's flexibility in dealing with multiple topologies. Two more examples showing the progression of the MVF active contour are shown in Fig. 6.

Broken boundary: Fig. 7 shows an example of the MVF active contour successfully recovering a shape with broken boundaries. None of other five methods could recover this S shape. The CF and CVF in particular require the object boundary to be connected.

The computation of the MVF field is a little more expensive than iteratively diffusing a gradient vector field (GGVF), but is generally much faster than constructing a CVF. For a 256×256 image, it takes about one minute to obtain the MVF on a 2.8GHz Pentium 4

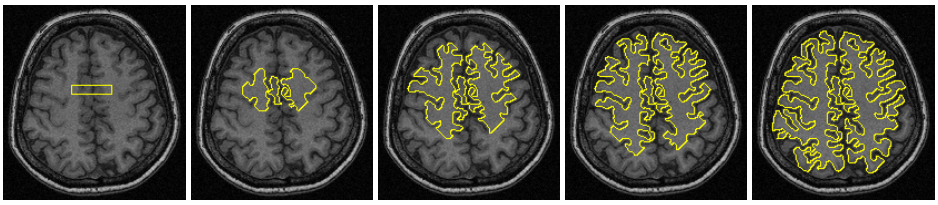

Figure 8: An example of applying MVF to real image.

with 1GB RAM (however, the software is written in Java and could be speeded up).

5 Conclusions

We proposed a novel external velocity field, MVF, for the active contour model. The flow is based on hypothesised magnetic interactions between the object boundary (or image gradients) and the active contour. The MVF can attract the contour into deep concave regions and does not suffer from saddle point and stationary point issues. Our comparative study showed a significant improvement in convergence capability on existing state-of-the-art techniques. As part of our future work, we plan to extend the MVF model to deal with real images. The key extension lies in the estimation of boundary orientation. For gray level images, we can perform this estimation directly based on image gradient vectors. Fig. 8 shows one initial result with very promising performance.

References

[1] V. Caselles, R. Kimmel, and G. Sapiro. Geodesic active contour. *IJCV*, 22(1):61–79, 1997.

[2] L. Cohen and I. Cohen. Finite-element methods for active contour models and balloons for 2-D and 3-D images. *IEEE T-PAMI*, 15(11):1131–1147, 1993.

[3] D. Gil and P. Radeva. Curvature vector flow to assure convergent deformable models for shape modelling. In *EMMCVPR*, pages 357–372, 2003.

[4] C. Li, J. Liu, and M. Fox. Segmentation of edge preserving gradient vector flow: an approach toward automatically initializing and splitting of snakes. In *CVPR*, pages 162–167, 2005.

[5] N. Paragios and R. Deriche. Geodesic active regions and level set methods for supervised texture segmentation. *IJCV*, 46(3):223–247, 2002.

[6] N. Paragios, O. Mellina-Gottardo, and V. Ramesh. Gradient vector flow geometric active contours. *IEEE T-PAMI*, 26(3):402–407, 2004.

[7] N. Ray and S. Acton. Motion gradient vector flow: External force for tracking rolling leukocytes with shape & size constrained active contours. *IEEE T-MI*, 23(12):1466–1478, 2004.

[8] K. Siddiqi, Y. Lauzière, A. Tannenbaum, and S. Zucker. Area and length minimizing flows for shape segmentation. *IEEE T-IP*, 7(3):433–443, 1998.

[9] D. Wolf. *Essentials of Electromagnetics for Engineering*. CUP, 2001.

[10] X. Xie and M. Mirmehdi. RAGS: Region-aided geometric snake. *IEEE T-IP*, 13(5):640–652, 2004.

[11] C. Xu and J. Prince. Generalized gradient vector flow external forces for active contours. *Signal Processing*, 71(2):131–139, 1998.

[12] C. Xu and J. Prince. Snakes, shapes, & gradient vector flow. *IEEE T-IP*, 7(3):359–369, 1998.